Plasma formation in fused silica induced by loosely focused femtosecond laser pulse

Alexander Q. Wu, Ihtesham H. Chowdhury, and Xianfan Xu[a)]
School of Mechanical Engineering, Purdue University, West Lafayette, Indiana 47907

(Received 27 June 2005; accepted 26 January 2006; published online 15 March 2006)

The focusing position inside fused silica irradiated by a loosely focused high power femtosecond laser pulse is studied both experimentally and numerically. The experimental measurement of plasma radiation shows that the laser pulse is focused behind the focal plane, which is also found in the numerical calculation and is attributed to a complex interplay between self-focusing due to the Kerr effect and defocusing because of the free electron plasma. Also, when more than one pulse is incident at the same spot in the sample, plasma radiation is observed at more than one spot along the laser propagation direction. © *2006 American Institute of Physics*. [DOI: 10.1063/1.2183361]

Femtosecond lasers have been proposed to micromachine transparent materials for fabricating waveguides,[1,2] optical gratings,[3,4] and other photonic devices.[5,6] These applications require a good understanding of the laser beam propagation and absorption inside the transparent materials. The dynamics of femtosecond laser propagation in transparent materials like fused silica is extremely complicated as the high intensity of the laser pulses leads to nonlinear effects such as self-focusing and creation of free electron plasma by nonlinear photoionization. Self-focusing occurs when the laser power exceeds a critical power P_{cr} and can lead to catastrophic damage.[7] The free-electron plasma leads to absorption of the pulse and also defocusing. The competition between these processes coupled with other effects like group velocity dispersion lead to rich pulse propagation phenomena such as pulse splitting,[8,9] filamentation,[10,11] and white light generation.[12] Plasma radiation perpendicular to the laser propagation direction has been used as a real-time measurement method to study the free electron distribution[13] and the optical breakdown in fused silica.[14,15] The experiments of optical breakdown shows that the laser beam is focused near the focal plane when the laser energy is not very high.[14,15]

In this letter, we report focusing behind the focal plane inside fused silica by loosely focused femtosecond laser pulses with high power, up to 500 times the self-focusing critical power $P_{cr} \sim 2$ MW. Such a laser condition is used, for example, for laser modification of internal structures of optical materials. Plasma radiation is measured and related to the calculated free electron distribution. The schematic of the experimental setup is shown in Fig. 1. A Spectra-Physics Spitfire regenerative amplifier system is used to produce 90 fs (full width at half maximum) pulses centered at 800 nm at a repetition rate of 0.5 kHz with a maximum energy of 1 mJ. An electronic shutter (Uniblitz LS6T2) is used to select single pulses and a half-wave-plate-polarizer combination is used to control the pulse energy. The pulses are loosely focused [i.e., using a small numerical aperture (NA)] inside fused silica by a 60 mm focal length lens, which is able to focus the laser beam into a 40 μm diam spot in air. The focal length along with the nominal beam diameter of 4 mm yields a NA of about 0.03. Samples are 6.35 mm thick fused silica (Corning 7980) which are optically polished on all sides. The samples are cleaned with methanol and acetone prior to laser irradiation and all the experiments are carried out in air at atmospheric pressure. The plasma radiation is observed from the side of the sample by using an imaging system consisting of a 0.28 NA long-working distance Mitutoyo 10X objective, a 200 mm focal length tube lens, and a charge coupled device camera. The camera is connected to a frame-grabber card on a computer to enable the acquisition of single-shot images. A filter is placed in front of the camera to block any scattered 800 nm light.

The numerical model used to compute femtosecond pulse absorption and propagation dynamics has been described in detail elsewhere.[16] Briefly, the linearly polarized laser pulse propagating is modeled using a 2(spatial) +1(temporal) dimensional wave propagation equation coupled with a rate equation for the free electron density. The generation of free electrons is predicted from the Keldysh theory which includes both multiphoton ionization and tunneling photoionization.[17] The propagation equation takes into account the effects of diffraction, group velocity dispersion, and laser energy absorption. Defocusing due to the free electron plasma and self-focusing because of the Kerr effect are simultaneously accounted for by computing the dielectric constant based on the Drude model. The equations are solved numerically using a Crank–Nicholson finite-differencing scheme to yield the spatial and temporal distribution of the laser intensity inside fused silica and the free electron densities.

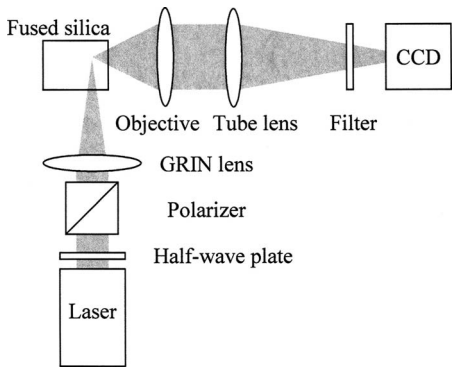

FIG. 1. Experimental setup for measurement of plasma radiation.

[a)]Electronic mail: xxu@ecn.purdue.edu

 © 2006 American Institute of Physics
Downloaded 13 Dec 2007 to 128.46.193.173. Redistribution subject to AIP license or copyright; see http://apl.aip.org/apl/copyright.jsp

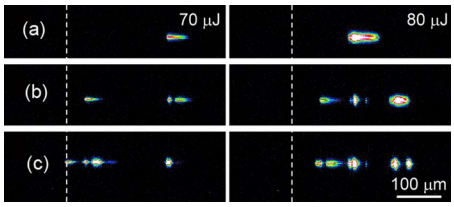

FIG. 2. (Color online) Experimental plasma radiation for the case of: (a) single pulse, (b) two pulses, and (c) three pulses with 70 and 80 μJ each incident on the same spot.

Figure 2 shows the recorded images of plasma radiation when the sample is irradiated by a single pulse [Fig. 2(a)], two pulses [Fig. 2(b)], and three pulses [Fig. 2(c)] with 70 and 80 μJ/pulse incident on the same spot. The laser pulse propagates from left to right in the image. The white dashed vertical lines represent the position of the focal plane in the absence of any nonlinear phenomena, which is behind the front surface at $z=1453$ μm (the sample surface is at $z=0$). Plasma radiation is seen at a position behind the focal plane, and it shifts forward with increase in incident laser energy.

Plasma formation behind the focal plan is due to the competition between the defocusing and self-focusing of the femtosecond pulse, which is also observed from the results of the numerical simulation of free electron density. Figures 3(a) and 3(b) represent the radial dependence of normalized time-integrated free electron density and normalized energy flux at four different positions along the laser propagation direction, with incident laser energy of 80 μJ/pulse. In the absence of any nonlinear effect, the laser beam diameter should remain almost constant inside the sample since under the focusing condition described above, the Rayleigh length is about 2.3 mm. However, it is seen that the laser pulse is defocused strongly near the surface—the beam is wider at $z=5$ μm than that at surface, $z=0$ μm. At $z=90$ μm, the Gaussian shape of the laser beam is distorted into a top-hat

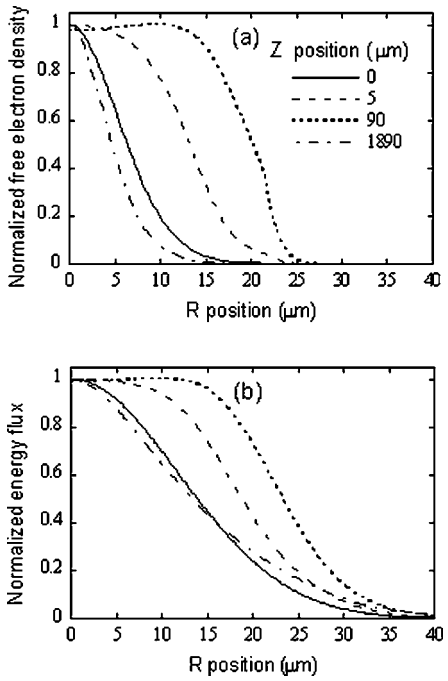

FIG. 3. Simulation results of normalized, radial position dependence of: (a) time integrated free electron density and (b) energy flux. The laser energy is 80 μJ/pulse.

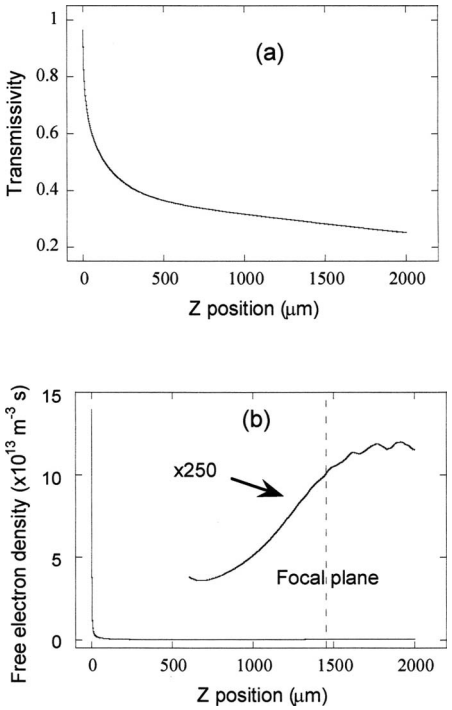

FIG. 4. Simulation results of z position dependence of (a) transmissivity and (b) time integrated free electron density at the beam center. The laser energy is 80 μJ/pulse.

shape. The defocusing is due to the dense free electron plasma[18] formed in the target. Figures 4(a) and 4(b) show the z position dependence of transmissivity, and the time integrated free electron density at the beam center. It is seen that very dense free electron plasma is formed close to the sample surface, and its density drops quickly within 5 μm because of the strong absorption and defocusing. For $z>90$ μm, the laser intensity as well as the free electron density are greatly reduced, leading to a focusing condition due to the dominant self-focusing effect and shrinkage of the laser beam diameter as shown in Fig. 3. The cumulative effect of defocusing and self-focusing results in the laser beam being focused behind the focal point as shown in Fig. 4(b), which shows the free electron density peaks behind the focal plane (the dashed vertical line, $z=1453$ μm). Note that the plot for $z>600$ μm is magnified by 250 times for clarity.

In order to further clarify the defocusing effect of the dense free electron plasma, Fig. 5 shows the image of time-integrated plasma radiation generated by a single pulse focused on the sample surface marked by the dashed white line. The incident laser energy is 80 μJ/pulse. Figure 5 clearly shows that the plasma is defocused strongly within 30 μm below the surface, although the Rayleigh length is around 2.3 mm. Some scattering of light, right to the dashed line, can be seen inside the fused silica. The radiation in air

FIG. 5. (Color online) Experimental plasma radiation of single pulse focused on sample surface with 80 μJ/pulse.

Downloaded 13 Dec 2007 to 128.46.193.173. Redistribution subject to AIP license or copyright; see http://apl.aip.org/apl/copyright.jsp

(left to the sample surface) is due to the expansion of the high dense plasma formed on the surface.

The above description of self-focusing and defocusing is qualitatively explained with the density of free electron plasma. In reality, there is complex interplay of self-focusing, defocusing, group velocity dispersion, and diffraction which are all considered in the numerical model. Experimentally, it is observed that the plasma radiation does occur at about 150 μm after the focal plane as shown in Fig. 2(a), and location of plasma formation moves forward as the laser energy increases. The simulation results are not compared with the experimental data quantitatively as both the detailed formation of plasma radiation from the free electron plasma and the effect of air on the laser beam propagation before the sample are not considered in the simulation model.

In experiments, it is also observed that when more than one pulse is incident at the same spot on the sample, plasma radiation occurs at more than one location inside the sample, resembling a filament broken up into multiple fragments. This is shown in Figs. 2(b) and 2(c) which show the plasma radiation measurements when the second and the third pulse hit the sample. The multiple plasma radiation spots can probably be attributed to the creation of defect states or damage by the preceding pulse inside the sample and the modification near the surface as the incident laser energy is above the damage threshold value. The subsequent pulses are absorbed more strongly in these positions leading to enhanced plasma radiation. This in turn leads to greater damage at these positions and therefore the plasma is observed to grow toward the surface of the sample when multiple pulses are allowed to hit the same spot.

In summary, the plasma radiation measurements and numerical simulation of free electron density revealed the complex nature of femtosecond pulse propagation in fused silica. Due to the various nonlinear effects like self-focusing of the Kerr effect and defocusing due to the free electron plasma, the laser pulse is focused behind the focal plane. It was also seen that in the case of irradiation with multiple pulses, the preceding pulses create defect and damage that can alter the absorption and propagation characteristics of the succeeding pulses.

Support of this work by the National Science Foundation and the Indiana 21st Century Research and Development Fund is gratefully acknowledged.

[1] A. M. Kowalevicz, V. Sharma, E. P. Ippen, J. G. Fujimoto, and K. Minoshima, Opt. Lett. **30**, 1060 (2005).
[2] A. Saliminia, N. T. Nguyen, M. C. Nadeau, S. Petit, S. L. Chin, and R. Vallee, J. Appl. Phys. **93**, 3724 (2003).
[3] Q. Wu, Y. Ma, R. Fang, Y. Liao, Q. Yu, X. Chen, and K. Wang, Appl. Phys. Lett. **82**, 1703 (2003).
[4] S. J. Mihailov, C. W. Smelser, D. Grobnic, R. B. Walker, P. Lu, H. M. Ding, and J. Unruh, J. Lightwave Technol. **22**, 94 (2004).
[5] M. Li, K. Mori, M. Ishizuka, X. Liu, Y. Sugimoto, N. Ikeda, and K. Asakawa, Appl. Phys. Lett. **83**, 216 (2003).
[6] M. Ventura, M. Straub, and M. Gu, Appl. Phys. Lett. **82**, 1649 (2003).
[7] R. W. Boyd, *Nonlinear Optics* (Academic, San Diego, 1992), Sec. 6.2.
[8] J. K. Ranka, R. W. Schirmer, and A. L. Gaeta, Phys. Rev. Lett. **77**, 3783 (1996).
[9] A. A. Zozulya, S. A. Diddams, A. G. Van Engen, and T. S. Clement, Phys. Rev. Lett. **82**, 1430 (1999).
[10] L. Sudrie, A. Couairon, M. Franco, B. Lamouroux, B. Prade, S. Tzortzakis, and A. Mysyrowicz, Phys. Rev. Lett. **89**, 186601 (2002).
[11] L. Berge, S. Skupin, F. Lederer, G. Mejean, J. Yu, J. Kasparian, E. Salmon, J. P. Wolf, M. Rodriguez, L. Woste, R. Bourayou, and R. Sauerbrey, Phys. Rev. Lett. **92**, 225002 (2004).
[12] A. L. Gaeta, Phys. Rev. Lett. **84**, 3582 (2000).
[13] Z. Wu, H. Jiang, Q. Sun, H. Yang, and Q. Gong, Phys. Rev. A **68**, 063820 (2003).
[14] N. T. Nguyen, A. Saliminia, W. Liu, S. L. Chin, and R. Vallée, Opt. Lett. **28**, 1591 (2003).
[15] A. Saliminia, N. T. Nguyen, S. L. Chin, and R. Vallée, Opt. Commun. **241**, 529 (2004).
[16] A. Q. Wu, I. H. Chowdhury, and X. Xu, Phys. Rev. B **72**, 085128 (2005).
[17] L. V. Keldysh, Sov. Phys. JETP **20**, 1307 (1965).
[18] S. C. Rae and K. Burnett, Phys. Rev. A **46**, 1084 (1992).

Downloaded 13 Dec 2007 to 128.46.193.173. Redistribution subject to AIP license or copyright; see http://apl.aip.org/apl/copyright.jsp